



Effective utilization of crustacean shells for preparing chitosan composite beads: applications in ameliorating the biosorption of an endocrine disrupting heavy metal

Muthulingam Seenuvasan^{a,*}, John Rini Gnana Suganthi^b, Gopalakrishnan Sarojini^a, George Carlin Geor Malar^c, Muzhumathi Ezhil Priya^d, Madhava Anil Kumar^a

^aDepartment of Petrochemical Engineering, SVS College of Engineering College, Coimbatore, India, email: msvasan.chem@gmail.com (M. Seenuvasan)

^bDepartment of Biotechnology, Madha Engineering College, Chennai, India

^cDepartment of Chemical Engineering, SSN College of Engineering, Chennai, India

^dDepartment of Chemical Engineering, Alagappa College of Technology, Anna University, Chennai, India

Received 3 March 2018; Accepted 17 March 2018

ABSTRACT

The study focuses on the removal of toxic hexavalent chromium (Cr(VI)) ions using fabricated chitosan composite beads (CCBs) using the shrimp shell waste and physically activated fish scales. The optimal parameters influencing biosorption were found to be pH 3.0, temperature 303 K, initial Cr(VI) concentration 100 mg/L after 150 min in batch experiments and the results showed 0.5 g CCBs adsorbed 99.86% Cr(VI). The Cr(VI) biosorption was confirmed using Fourier transform infrared spectroscopy analyses. The equilibrium data were fit into different isotherms such as Freundlich, Langmuir, Temkin, and Dubinin–Radushkevich (D-R) models to elucidate Cr(VI) biosorption onto CCBs. The equilibrium results suggested that the biosorption was a physical process. The maximum adsorption capacity (q_e) of CCBs was 28.9 mg/g and the pseudo-second-order kinetics best described the adsorption kinetics. Furthermore, the feasibility of CCBs regeneration using suitable treatment demonstrated desorption of Cr(VI) ions economically.

Keywords: Biosorption; Crustacean shells; Chitosan composite beads; Regeneration

1. Introduction

Heavy metal pollution is a serious threat to biotic components of the ecosystem; as they exhibit toxicity even at low concentration and tend to bioaccumulate causing severe health problems [1]. Natural processes and anthropogenic industrial activities release Cr(VI) ions that cause severe deterioration of environmental health as they are reported carcinogens [2]. Hence, it is mandatory that the industries to reduce the release of Cr(VI) to an acceptable level. In order to reduce the heavy metal concentration in the aquatic

ecosystems, various treatment methods are employed such as bioremediation, precipitation, photo-catalysis, ion exchange, and membrane processes [3,4]. However, application of some of these methods may be impractical due to economic constraints or may be insufficient to meet the stringent regulations and furthermore, they generate hazardous products [5,6].

Biosorption is pervasively used to reduce the metal contaminants in surface water and industrial effluents [7]. Adsorbents such as activated carbon and ion-exchange resins are of high cost and thus, the renewable materials can be used as adsorbents [8]. Chitin and chitosan are the two

* Corresponding author.

Presented at the 3rd International Conference on Recent Advancements in Chemical, Environmental and Energy Engineering, 15–16 February, Chennai, India, 2018.

promising biopolymers prepared from waste crustacean shells and are reported to adsorb distinct heavy metals. This may be attributed to the reason that they have high proportion of nitrogen sites available with greater affinity for the metal ions [9,10].

In the present study, chitosan composite beads (CCBs) were fabricated by utilizing the crustaceans' shells and were employed to adsorb Cr(VI). Also, to explore the degree of deacetylation and to study the effect of process parameters influencing biosorption. The biosorption equilibrium and kinetic behaviour were assessed with the help of different models and Cr(VI) desorption to be elucidated for the successful regeneration of CCBs.

2. Materials and methods

2.1. Chemicals and shell waste of crustaceans

Hydrochloric acid, acetone, sulphuric acid, 1,5-diphenyl-carbazide, glacial acetic acid, ethylenediaminetetraacetic acid (EDTA), potassium dichromate and nitric acid were purchased from Navakar Bio Chemicals (Chennai, India). Glutaraldehyde (GA) 25% (w/v) was the guaranteed reagent from Loba Chemie Pvt. Ltd. (Mumbai, India). Sodium tripolyphosphate (TPP) was purchased from Sisco Research Laboratories Pvt. Ltd. (India). A stock solution (500 mg/L) of Cr was prepared by dissolving potassium dichromate in deionized water and was stored at room temperature. The shrimp shells waste and fish scales were collected from the local market. All the chemicals were of highest purity and analytical grade.

2.2. Synthesis of chitosan

200 g of crustacean shells were washed thoroughly, sun-dried for 48 h and was ground to powder. The demineralization was accomplished by treating the shell powder with 5% HCl in the ratio of 1:6 (w/v) for 24 h at room temperature followed by rinsing and drying. The process was repeated until complete demineralization and the demineralized powder was subjected to alkali treatment with 5% NaOH in the ratio of 1:10 (w/v) at 343 K for 48 h. The processed shells were washed, sun-dried to yield chitin and was converted to chitosan (deacetylation) by removal of acetyl group by treating the chitin with 60% NaOH in the ratio 1:15 (w/v) followed by heating for 2 h. The resultant chitosan was then rinsed and dried at 333 K.

2.3. Fabrication of chitosan composite beads

The solution of 1.0% chitosan along with 1.0 g of processed fish scales [11] in 2.0% acetic acid was stirred vigorously overnight, and left still for 6 h. 100 mL of chitosan solution was dropped into 1,000 mL of reducing reagent (10% NaOH and ethanol in the ratio of 4:1) and the beads obtained by using 1.0% TPP were found to be more stable. The resultant beads were filtered, rinsed with distilled water. CCBs were then cross-linked using (1:1 w/v) GA and the beads were filtered, rinsed with distilled water and kept in deionized water until use.

2.4. Biosorption experiments

The batch biosorption was performed with Cr(VI) ion solution in different concentrations (10–250 mg/L). To the metal solution, 0.5 g CCBs were added and agitated at a constant speed for 150 min at 305 ± 2 K. The influence of pH (2.0–8.0), initial concentration (10, 25, 50, 75, 100, 150, 200, and 250 mg/L), contact time (30–240 min), adsorbent dose (0.1–0.7 g), and temperature (293, 303, 313, 323, 333, and 343 K) was evaluated. At predetermined time intervals, the samples were withdrawn and the residual concentration and uptake of Cr(VI) ion was quantified by UV-Visible absorption spectrophotometer (U3210, Hitachi, Japan). The adsorption of Cr(VI) ions onto the CCBs was confirmed by Fourier transform infrared (FTIR) spectra recorded on a Perkin Elmer 237B Infrared spectrometer.

3. Results and discussion

3.1. Fabrication of CCBs and efficacy of CCBs for Cr(VI) biosorption

The metal sorption capacity of chitosan varies with crystallinity, affinity of water, deacetylation degree, and amino group content. Also, the chitosan exhibited higher sorption capacities in bead form when compared with the other forms [12]. The percentage yield of chitosan from the flaky structures of the crustacean shells was found to be 11.05% and the degree of deacetylation [13] was found to be 78.87% determined by titrating chitosan solution against sodium hydroxide (equivalence point was observed at pH 3.0).

The ability of the fabricated CCBs in adsorbing the Cr(VI) from aqueous solution was tested in 100 mL of reaction containing 100 mg/L Cr(VI) onto 0.5 g/L CCBs at 200 rpm for a span of 2 h. The aliquots were quantified for the residual Cr(VI) concentration and the biosorption onto CCBs was confirmed by recording the FTIR spectra (Fig. 1) of CCBs before and after Cr(VI) biosorption. The spectra of CCBs showed characteristic peak at 3445 cm^{-1} for the stretching vibrations of hydroxyl and free amino groups. The presence of amide I and II groups was confirmed by the peaks at 1,646

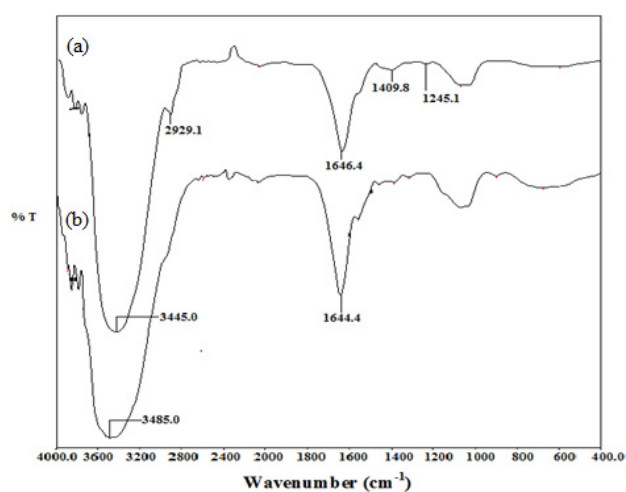


Fig. 1. FTIR spectra of CCBs before (a) and after (b) adsorption of Cr(VI).

and $1,409\text{ cm}^{-1}$, respectively, and the CO stretching vibration was observed at $1,245\text{ cm}^{-1}$. After Cr(VI) biosorption, the characteristic peak at $2,929\text{ cm}^{-1}$ corresponding to typical CH stretching vibration was not observed conforming the intermolecular hydrogen bond formation with metal ions.

3.2. Effect of initial Cr(VI) concentration

The % biosorption was found to decrease for increased Cr(VI) concentration (Fig. 2), which may be attributed to the reason that only limited active sites were available on the CCBs to adsorb Cr(VI) ions [14]. Conversely, the value of q_e (mg/g) increased with the increase in the initial Cr(VI) concentration (Fig. 2), which could be because of the reason that initial concentration of Cr(VI) offered much driving force to overcome the mass transfer resistance between the solid and aqueous phase [15].

3.3. Effect of agitation time

The agitation time refers to the time at which the system attains the equilibrium before the adsorption becomes constant. Initially, Cr(VI) biosorption was found to be high (Fig. 3) since biosorption is the effect of higher diffusion rate of the adsorbate into the intraparticle pores of the adsorbent and the equilibrium state was achieved after 150 min.

3.4. Effect of temperature

The Cr(VI) biosorption was found to be maximum at 303 K and decreased when the temperature was raised beyond 303 K (Fig. 4) and this phenomenal decrease in the biosorption may be due to the reason that the higher temperature enhanced the mobility of the adsorbate causing desorption.

3.5. Effect of pH

The maximum biosorption was observed at pH 2.0 and the efficiency decreased at higher pH as shown in Fig. 5. The higher pH levels ruptured the internal hydrogen bonds, which resulted in the swelling of CCBs and also by the protonation of amino groups [16].

3.6. Effect of adsorbent dosage

Fig. 6 shows the effect of adsorbent dosage on q_e and % biosorption where the CCBs dose was varied from 0.1 to 0.7 g/L and the biosorption capacity reduced from 64.87 to 14.257 mg/g and this reduction in biosorption may be due to the result of increase in the surface area available for the Cr(VI) biosorption. The maximum biosorption was 99.86% and observed that when the system was supplied with 0.5 g/L CCBs and further increase in the dose did not exhibit any significant change in biosorption and this may be due to the non-availability of anymore free active sites.

3.7. Pre-equilibrium kinetics of biosorption of Cr(VI) onto CCBs

The kinetics mechanism involved in Cr(VI) ion adsorption was investigated using many possible kinetic models such as

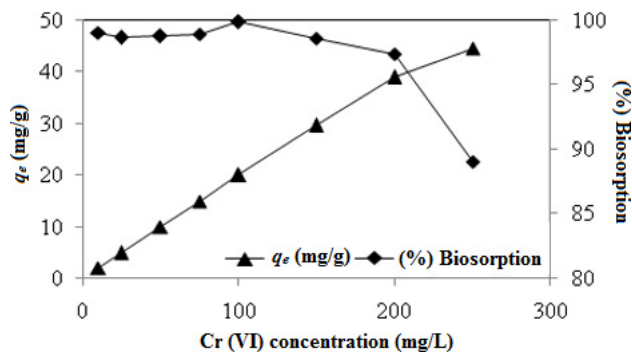


Fig. 2. Effect of initial Cr(VI) concentration on q_e and % biosorption.

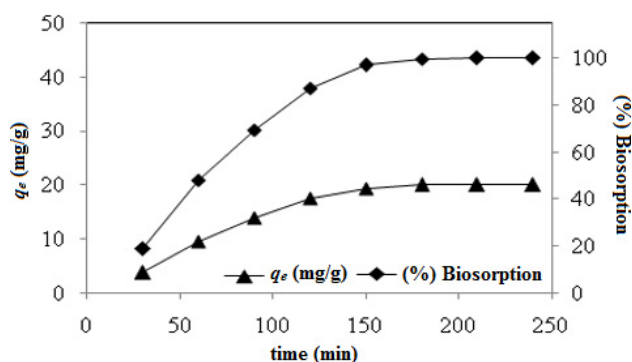


Fig. 3. Effect of agitation time on q_e and % biosorption.

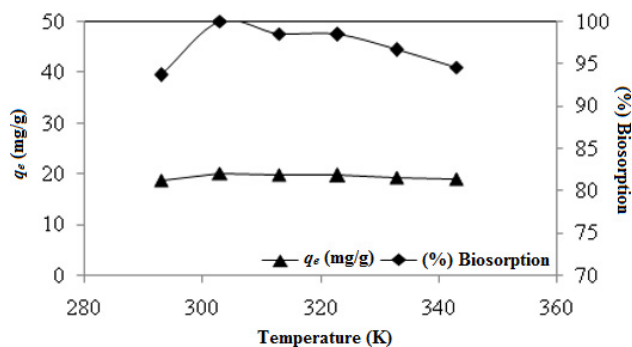


Fig. 4. Effect of temperature on q_e and % biosorption.

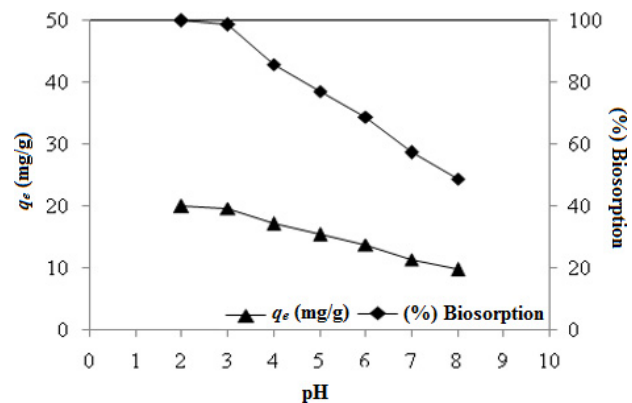


Fig. 5. Effect of pH on q_e and % biosorption.

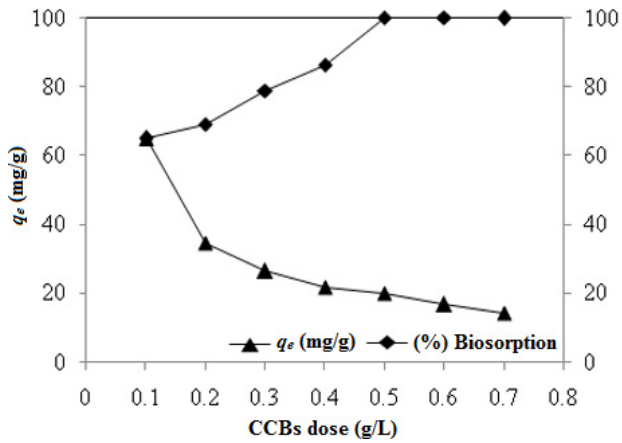


Fig. 6. Effect of adsorbent dosage on q_e and % biosorption.

first-order, pseudo-first-order, pseudo-second-order, Elovich relations, and intraparticle diffusion model. Based on the experimental data and the model, predicted values were expressed by the correlation coefficient (R^2). The model with relatively higher R^2 values describes the kinetics of Cr(VI) ion adsorption successfully. First, the simple first-order rate kinetics [17] given by Eq. (1):

$$\log C_e = \frac{k_1}{2.303}t + \log C_0 \quad (1)$$

where C_0 and C_e are the concentration of metal ion at initial and at time t (mg/L) respectively, and k_1 is the first-order rate constant (1/min). Fig. 7(a) depicts the plot of $\log C_e$ vs. t for constant initial concentration of metal ions from which the rate constant and correlation coefficient were obtained. The deviation in

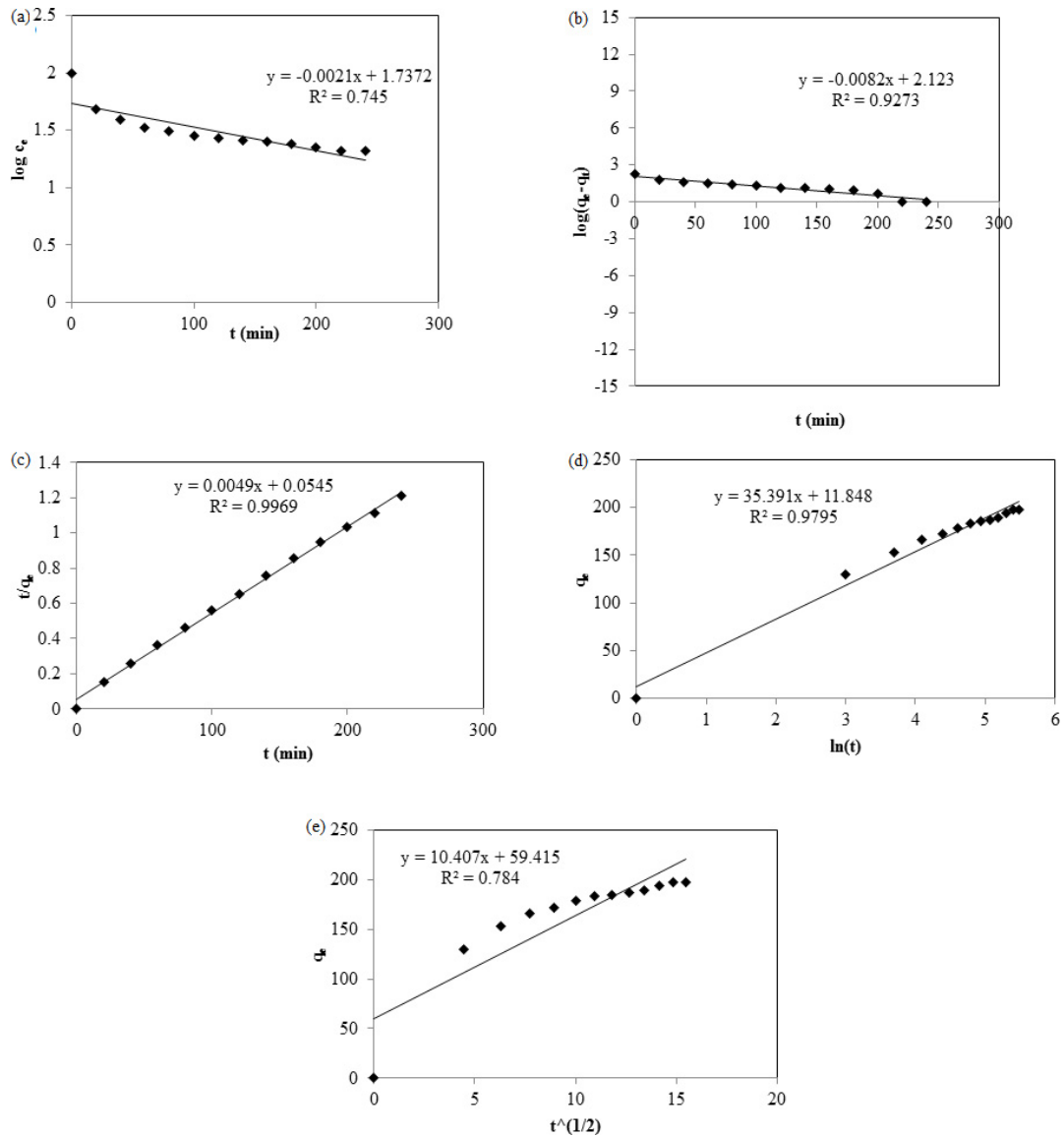


Fig. 7. Kinetic models (a) first-order, (b) pseudo-first-order, (c) pseudo-second-order, (d) Elovich, (e) intraparticle diffusion and their statistical parameters at pH = 3.0, $T = 305 \pm 2$ K, $C_0 = 100$ mg/L, 0.5 g CCBs, and 200 rpm.

theoretical data indicates the failure in expressing the adsorption process by the simple first-order kinetics.

Second, the adsorption kinetics was investigated using the linear form of pseudo-first-order kinetics [18] as given by Eq. (2):

$$\log(q_0 - q_e) = \log(q_0) - \frac{k_1}{2.303}t \quad (2)$$

where q_0 and q_e are the metal ion concentration at equilibrium and at time t (mg/g), and k_1 is the rate constant for pseudo-first-order kinetics (1/min). The rate constant and correlation coefficient were evaluated from the slope and intercept of the plot between $\log(q_0 - q_e)$ and t (Fig. 7(b)).

Third, the pseudo-second-order kinetics [19] was determined by Eq. (3):

$$\frac{t}{q_e} = \frac{1}{k_2 q_0^2} + \frac{t}{q_0} \quad (3)$$

where k_2 is the rate constant of second-order adsorption (g/mg min). The plot of t/q_e against t (Fig. 7(c)) is a linear fit and also on comparison, highest R^2 value of 0.99 was observed, which jointly suggests the applicability of this kinetic model for the system. It can be confirmed that the Cr(VI) ion adsorption process follows the pseudo-second-order kinetics.

Fourth, the linearized Elovich equation [20] can be expressed as given in Eq. (4):

$$q_t = \frac{\ln a_e b_e}{b_e} + \frac{1}{b_e} \ln t \quad (4)$$

where a_e and b_e are the initial adsorption rate (mg/g min) and adsorption constant (g/mg), respectively. Fig. 7(d) shows the plot of $\ln t$ vs. q and the parameters were calculated from the slope and intercept of the plot. The R^2 value was found to be 0.97.

Finally, the intraparticle diffusion [21] can be described by the following Eq. (5):

$$q = k_i t^{0.5} + C \quad (5)$$

where k_i is the intraparticle diffusion rate constant (mg/g h^{0.5}), C is the intercept. Fig. 7(e) depicts the intraparticle diffusion

model graphically from which the correlation coefficient value was found to be 0.76. Table 1 gives the complete comparison of kinetic parameters of all the kinetic models.

3.8. Equilibrium biosorption isotherm studies

The equilibrium data for the biosorption of Cr(VI) onto CCBs were analyzed (Table 2) using two parameter isotherm models such as Langmuir, Freundlich, Temkin, and Dubinin–Radushkevich (D-R). Langmuir adsorption isotherm model [22] is valid for monolayer adsorption onto a surface containing finite number of identical sites. Thereby, the equilibrium distance between the metal ion in the solution and the liquid phases can be represented by Langmuir. The model assumes uniform energies of adsorption onto the surface and no transmigration of adsorbate in the plane of surface. Eq. (6) represents the Langmuir isotherm:

$$\frac{1}{q_e} = \frac{1}{Q_0} + \frac{1}{Q_0 K_L C_e} \quad (6)$$

where q_e is the amount of metal adsorbed per gram of the adsorbate at equilibrium (mg/g), Q_0 is the maximum monolayer coverage capacity (mg/g), K_L is the Langmuir isotherm constants (L/mg), and C_e is the equilibrium concentration of the adsorbate (mg/L). The values of Q_0 and K_L were computed from the slopes and intercepts of Langmuir

Table 1

Kinetic models and their statistical parameters at pH = 3.0, $T = 305 \pm 2$ K, $C_0 = 100$ mg/L, 0.5 g CCBs, and 200 rpm

Kinetic model	Parameters	
First-order equation	R^2	0.745
	k_1 (1/min)	0.0048
Pseudo-first-order equation	R^2	0.9273
	k_1 (1/min)	0.0189
Pseudo-second-order equation	R^2	0.9969
	k_2 (g/mg min)	0.000441
Elovich model	R^2	0.9795
	A	49.76
	B	0.028
Intraparticle diffusion model	R^2	0.784
	k_i (mg/g h ^{0.5})	10.407

Table 2

Equilibrium biosorption isotherms for Freundlich, Langmuir, Temkin, and Dubinin–Radushkevich isotherm models at pH = 3.0, $T = 305 \pm 2$ K, $C_0 = 100$ mg/L, 0.5 g CCBs, and 200 rpm

Langmuir			Freundlich			
Q_0 (mg/g)	R_L	R^2	n	K_f (mg/g)	R^2	
28.9	0.208	0.9929	1.416	0.8776	0.9911	
Temkin			Dubinin–Radushkevich			
A_T (L/mg)	b (J/mol)	R^2	q_s (mg/g)	K_{ad} (mol ² /kJ ²)	E (kJ/mol)	R^2
0.1686	7.038	0.9235	15.105	2×10^{-5}	158.11	0.8105

plot of $1/q_e$ vs. $1/C_e$ as shown in Fig. 8(a). The value of R_L decides the type of isotherm and it was determined (Eq. (7)) to be less than 1, which indicates that Langmuir isotherm is suited for the adsorption of Cr(VI) by CCBs [23].

$$R_L = \frac{1}{1+(1+K_L C_0)} \quad (7)$$

Freundlich adsorption isotherm [24] is tested to check the affinity between adsorbate and adsorbent [17]. Eq. (8) explains the linearized equation of Freundlich isotherm.

$$\log q_e = \log K_f + \frac{1}{n} \log C_e \quad (8)$$

where K_f is the Freundlich isotherm (mg/g), n is the adsorption intensity, C_e is the equilibrium concentration of the adsorbate (mg/L), and q_e is the amount of metal adsorbed per gram of adsorbate at equilibrium (mg/g). The constant K_f is an indicator of adsorption capacity, while $1/n$ is a function of strength of adsorption in adsorption process [7], which was found by linear plot as shown in Fig. 8(b). From the data obtained, the value of $1/n$ was 0.706 and the value of n was found to be greater than unity ($n = 1.416$) confirming higher affinity between the Cr(VI) and CCBs [25].

Temkin isotherm [26] accounts to be adsorbent–adsorbate interactions by ignoring extremely low and high values of the concentration. According to this model, the heat of the adsorption of all molecules in the layer would decrease

linearly rather than logarithmic with average [2,12]. It was carried out by plotting the quantity adsorbed q_e against $\ln C_e$ and the constants were found from the slope and the intercept. The isotherm [27] is given by Eq. (9):

$$q_e = \frac{RT}{b} \ln(A_T C_e) \quad (9)$$

where A_T is the Temkin isotherm equilibrium binding constant (L/g), R is the universal gas constant (8.314 J/mol K), T is the temperature at 298 K, and b is the constant related to heat of sorption (J/mol). The heat of sorption (b) and A_T values were calculated to be 7.038 J/mol and 0.1686 L/mg from the slope and the intercept of linearized Temkin plot (Fig. 8(c)), which indicates that it was a physical adsorption process.

Dubinin–Radushkevich isotherm [28] model often fits high solute activities and the intermediate range of concentration data. The isotherm can be expressed by Eq. (10):

$$q_e = q_s \exp(-k_{ad} \varepsilon^2) \quad (10)$$

where q_e is the amount of adsorbate in the adsorbent at equilibrium (mg/g) and k_{ad} is the D-R isotherm constant (mol^2/kJ^2). From the plot of the isotherm (Fig. 8(d)), q_s was found to be 15.105 mg/g. This model was used to distinguish the process of adsorption of Cr(VI) ions and the value of E (158.11 KJ/mol) indicated it was a physical adsorption process.

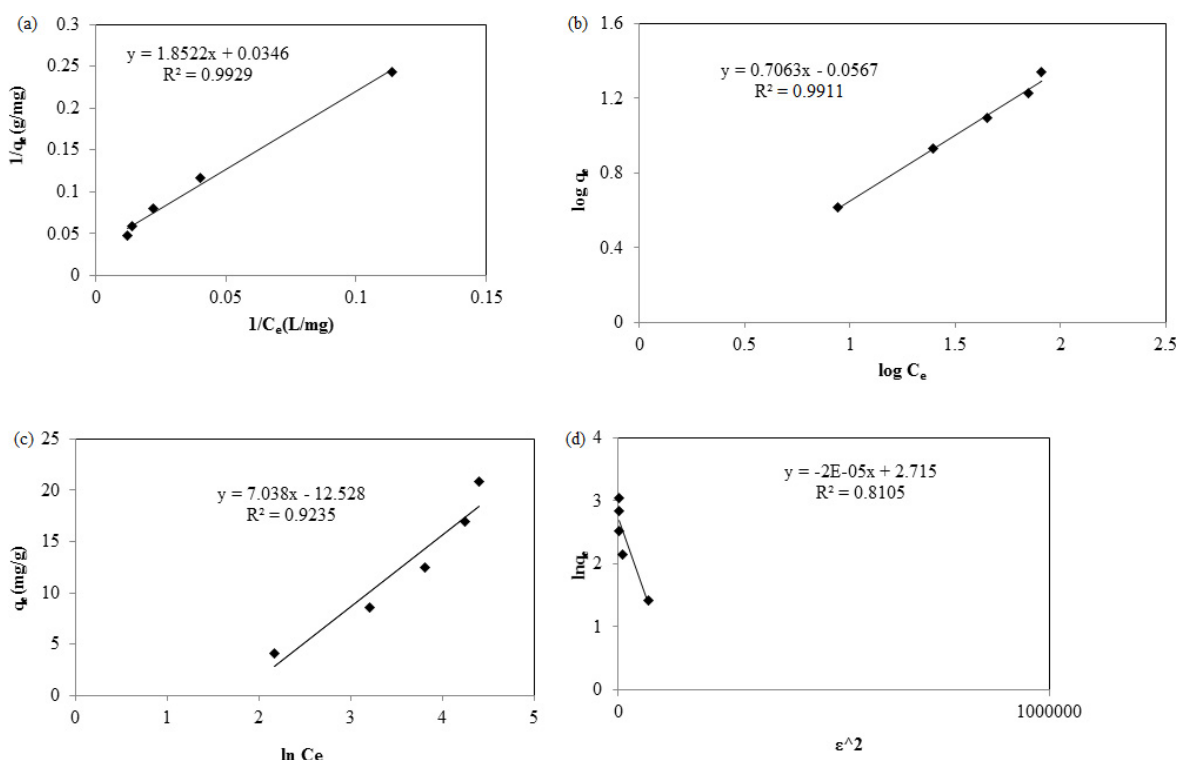


Fig. 8. Equilibrium modeling (a) Langmuir isotherm, (b) Freundlich isotherm, (c) Temkin isotherm, (d) Dubinin–Radushkevich isotherm plots for adsorption of Cr(VI) on CCBs.

Table 3
Percentage desorption of Cr(VI) from the CCBs biosorbed with Cr(VI)

Chemical	Concentration (M)	Desorption (%)
EDTA	1×10^{-2}	93.5
	1×10^{-3}	76.9
	1×10^{-4}	53.8
HNO ₃	1×10^{-2}	82.7
	1×10^{-3}	69.3
	1×10^{-4}	41.2

The isotherm constants and correlation coefficients (R^2) were presented in Table 2. The slightly higher in R^2 value for Langmuir as compared with other isotherm models indicated the perfect fit of Langmuir isotherm model than other models, confirming the homogenous surface of the CCBs.

3.9. Regeneration of CCBs

The recovery and regeneration of adsorbent are an important aspect and top prioritized criterion for the economic feasibility for running the operation [29,30]. The regeneration of CCBs was done by desorbing the biosorbed Cr(VI) using appropriate chemical treatment using EDTA and nitric acid (HNO₃) at varying concentrations. CCBs tend to solubilize in EDTA and HNO₃ at higher concentration and the percentage Cr(VI) desorption from the CCBs are listed in Table 3. The desorption efficiency was greater in case of desorption aided with EDTA than HNO₃ as the EDTA is a hexadentate chelating agent and is capable of forming complexes with Cr(IV).

4. Conclusions

The present study revealed that the CCBs prepared from shrimp shell wastes and fish scales were a suitable and efficient biosorbent for the adsorption of Cr(VI) ions. The adsorption capacity of CCBs was investigated to be 34.52 mg/g. Maximum removal with 99.86% of Cr(VI) ions was observed at pH 3.0, adsorbent dosage of 0.5 g, agitation time of 150 min. The mathematical description of biosorption of Cr(VI) ions onto CCBs was studied by the Freundlich, Langmuir, Temkin, and Dubinin–Radushkevich isotherm models. Out of which, the Langmuir isotherm was found to be best fit for the adsorption process with R^2 value of 0.9921; Temkin and Dubinin–Radushkevich isotherm models showed it was a physisorption process. Batch equilibrium suggested that the system followed pseudo-second-order kinetics. The successful adsorption of Cr(VI) ions on the CCBs was further confirmed by FTIR analysis. CCBs were regenerated using desorption studies with EDTA that would enhance the economy of practical applications for the removal of Cr(VI) ions from the water and wastewater.

References

- [1] P.S. Kumar, K. Kirthika, K.S. Kumar, Removal of hexavalent chromium ions from aqueous solutions by an anion-exchange resin, *Adsorpt. Sci. Technol.*, 26 (2008) 693–703.
- [2] N. Saranya, E. Nakeeran, M.S.G. Nandagopal, N. Selvaraju, Optimization of adsorption process parameters by response surface methodology for hexavalent chromium removal from aqueous solutions using *Annona reticulata* Linn peel microparticles, *Water Sci. Technol.*, 75 (2017) 2094–2107.
- [3] S. Karthikeyan, M.A. Kumar, P. Maharaja, B.P. Rao, G. Sekaran, Process optimization for the treatment of pharmaceutical wastewater catalyzed by poly sulphur sponge, *J. Taiwan Inst. Chem. Eng.*, 45 (2014) 1739–1747.
- [4] S. Rangabhashiyam, N. Anu, N. Selvaraju, Equilibrium and kinetic modeling of chromium (VI) removal from aqueous solution by a novel biosorbent, *Res. J. Chem. Environ.*, 18 (2014) 30–36.
- [5] E. Nakkeeran, N. Saranya, M.S.G. Nandagopal, A. Santhiagu, N. Selvaraju, Hexavalent chromium removal from aqueous solutions by a novel powder prepared from *Colocasia esculenta* leaves, *Int. J. Phytorem.*, 18 (2016) 812–821.
- [6] E. Nakkeeran, S. Rangabhashiyam, M.S.G. Nandagopal, N. Selvaraju, Removal of Cr(VI) from aqueous solution using *Strychnos nux-vomica* shell as an adsorbent, *Desal. Wat. Treat.*, 57 (2016) 23951–23964.
- [7] T. Vidhyadevi, A. Murugesan, S.S. Kalaivani, M.A. Kumar, K.V.T. Ravi, L. Ravikumar, C.D. Anuradha, S. Sivanesan, Optimization of the process parameters for the removal of reactive yellow dye by the low cost *Setaria verticillata* carbon using response surface methodology: thermodynamic, kinetic and equilibrium studies, *Environ. Prog. Sustain. Energy*, 33 (2014) 855–865.
- [8] U.P. Kiruba, P.S. Kumar, K.S. Gayatri, S.S. Hameed, M. Sindhuja, C. Prabhakaran, Study of adsorption kinetic, mechanism, isotherm, thermodynamic and design models for Cu(II) ions on sulphuric acid modified Eucalyptus seeds: temperature effect, *Desal. Wat. Treat.*, 56 (2015) 2948–2965.
- [9] K. Anbalagan, P.S. Kumar, K.S. Gayatri, S.S. Hameed, M. Sindhuja, C. Prabhakaran, R. Karthikeyan, Removal and recovery Ni(II) ions from synthetic wastewater using surface modified *Strychnos potatorum* seeds: experimental optimization and mechanism, *Desal. Wat. Treat.*, 53 (2015) 171–182.
- [10] D. Prabu, R. Parthiban, P.S. Kumar, N. Kumari, P. Saikia, Adsorption of copper ions onto nano scale zero-valent iron impregnated cashew nut shell, *Desal. Wat. Treat.*, 57 (2016) 6487–6502.
- [11] M. Seenivasan, K.S. Kumar, G.C.G. Malar, S. Preethi, M.A. Kumar, N. Balaji, Characterization, analysis, and application of fabricated Fe₃O₄-chitosan-pectinase nanobiocatalyst, *Appl. Biochem. Biotechnol.*, 172 (2014) 2706–2719.
- [12] S. Rangabhashiyam, E. Suganya, A.V. Lity, N. Selvaraju, Equilibrium and kinetics studies of hexavalent chromium biosorption on a novel green macroalgae *Enteromorpha* sp., *Res. Chem. Intermed.*, 42 (2016) 1275–1294.
- [13] K. Anbalagan, P.S. Kumar, R. Karthikeyan, Adsorption of toxic Cr(VI) ions from aqueous solution by sulphuric acid modified *Strychnos potatorum* seeds in batch and column studies, *Desal. Wat. Treat.*, 57 (2016) 12585–12607.
- [14] T. Anitha, P.S. Kumar, K.S. Kumar, K. Sriram, J.F. Ahmed, Biosorption of lead(II) ions onto nano-sized chitosan particle blended polyvinyl alcohol (PVA): adsorption isotherms, kinetics and equilibrium studies, *Desal. Wat. Treat.*, 57 (2016) 13711–13721.
- [15] A. Saravanan, P.S. Kumar, B. Preetha, Optimization of process parameters for the removal of chromium(VI) and nickel(II) from aqueous solutions by mixed biosorbents (custard apple seeds and *Aspergillus niger*) using response surface methodology, *Desal. Wat. Treat.*, 57 (2016) 14530–14543.
- [16] T. Anitha, P.S. Kumar, K.S. Kumar, B. Ramkumar, S. Ramalingam, Adsorptive removal of Pb(II) ions from polluted water by newly synthesized chitosan-polyacrylonitrile blend: equilibrium, kinetic, mechanism and thermodynamic approach, *Process Saf. Environ. Prot.*, 98 (2015) 187–197.
- [17] A. Saravanan, K.A. Kumar, R. Yashwanth, S. Visvesh, P.S. Kumar, Removal of toxic zinc from water/wastewater using eucalyptus seeds activated carbon: non-linear regression analysis, *IET Nanobiotechnol.*, 10 (2016) 244–253.
- [18] Y.S. Ho, Citation review of Lagergren kinetic rate equation on adsorption reactions, *Scientometrics*, 59 (2004) 171–177.

- [19] Y.S. Ho, Second-order kinetic model for the sorption of cadmium onto tree fern: a comparison of linear and non-linear methods, *Water Res.*, 40 (2006) 119–125.
- [20] M.J.D. Low, Kinetics of chemisorption of gases on solids, *Chem. Rev.*, 60 (1960) 267–312.
- [21] W.J. Weber, J.C. Morris, Kinetics of adsorption on carbon from solution, *J. Sanit. Eng. Div.*, 89 (1963) 31–60.
- [22] K. Nithya, A. Sathish, P.S. Kumar, T. Ramachandran, Biosorption of hexavalent chromium from aqueous solution using raw and acid treated biosorbent prepared from *Lantana camara* fruit, *Desal. Wat. Treat.*, 57 (2016) 25097–25113.
- [23] S. Suganya, K. Kayalvizhi, P.S. Kumar, A. Saravanan, V.V. Kumar, Biosorption of Pb(II), Ni(II) and Cr(VI) ions from aqueous solution using *Rhizoclonium tortuosum*: extended application to nickel plating industrial wastewater, *Desal. Wat. Treat.*, 57 (2016) 25114–25139.
- [24] M.A. Kumar, V.V. Kumar, M.P. Premkumar, P. Baskaralingam, K.V. Thiruvengadaravi, D. Anuradha, S. Sivanesan, Chemometric formulation of bacterial consortium-AVS for improved decolorization of resonance-stabilized and heteropolyaromatic dye, *Bioresour. Technol.*, 123 (2012) 344–351.
- [25] T.V. Novi, V.V. Kumar, P.S. Kumar, C. Christy, S.S. Lavanyaa, D. Vishnu, A. Saravanan, V.V. Kumar, S. Sivanesan, Review on nano adsorbents: a solution for heavy metal removal from wastewater, *IET Nanobiotechnol.*, 11 (2017) 213–224.
- [26] M. Temkin, V. Pyzhev, Kinetics of ammonia synthesis on promoted iron catalysts, *Acta Physicochimica U.R.S.S.*, 12 (1940) 217–222.
- [27] E. Gunasundari, P.S. Kumar, Higher adsorption capacity of *Spirulina platensis* alga for Cr(VI) ions removal: parameter optimization, equilibrium, kinetic and thermodynamic predictions, *IET Nanobiotechnol.*, 11 (2017) 317–328.
- [28] M.M. Dubinin, The potential theory of adsorption of gases and vapors for adsorbents with energetically nonuniform surfaces, *Chem. Rev.*, 60 (1960) 235–241.
- [29] A. Saravanan, P.S. Kumar, M. Yashwanthraj, Sequestration of toxic Cr(VI) ions from industrial wastewater using waste biomass: a review, *Desal. Wat. Treat.*, 68 (2017) 245–266.
- [30] G. Neeraj, S. Krishnan, P.S. Kumar, K.R. Shriaishvarya, V.V. Kumar, Performance study on sequestration of copper ions from contaminated water using newly synthesized high effective chitosan coated magnetic nanoparticles, *J. Mol. Liq.*, 214 (2016) 335–346.